

Lawrence Berkeley National Laboratory

Lawrence Berkeley National Laboratory

Title

New ion-guide for the production of beams of neutron-rich nuclei between $Z = 20 - 28$

Permalink

<https://escholarship.org/uc/item/96s4p5pr>

Authors

Perajarvi, Kari
Cerny, Joe
Hakala, Jani
et al.

Publication Date

2004-12-08

Peer reviewed

New ion-guide for the production of beams of neutron-rich nuclei between $Z = 20 - 28$

K. Peräjärvi^{1*}, J. Cerny^{1,2}, J. Hakala³, J. Huikari³, A. Jokinen³, P. Karvonen³, J. Kurpeta⁴, D. Lee^{1,5}, I. Moore³, H. Penttilä³, A. Popov⁶ and J. Äystö³

¹ Nuclear Science Division, Lawrence Berkeley National Laboratory, Berkeley, CA 94720, USA

² Department of Chemistry, University of California, Berkeley, CA 94720, USA

³ Department of Physics, P.O. Box 35, FIN-40014 University of Jyväskylä, Finland

⁴ University of Warsaw, PL-00681 Warsaw, Poland

⁵ Department of Nuclear Engineering, University of California, Berkeley, CA 94720, USA

⁶ St. Petersburg Nuclear Physics Institute, Gatchina, 188350, Russia

Abstract

It has been shown for the first time that quasi- and deep-inelastic reactions can be successfully incorporated into the conventional Ion-Guide Isotope Separator On-Line (IGISOL) technique. This is of particular interest for characterizing the decay properties of refractory elements and is applied to neutron rich nuclei between $Z = 20 - 28$. As a first step of this project, the kinematics of quasi- and deep-inelastic reactions, such as $^{197}\text{Au}(^{65}\text{Cu},\text{X})\text{Y}$, were studied. Based on these studies, a specialized IGISOL target chamber was designed and built. This chamber was tested in on- and off-line conditions at the Jyväskylä IGISOL facility. Yields of radioactive, projectile-like species such as $^{62,63}\text{Co}$ are about 0.8 ions/s/pnA corresponding to a total IGISOL efficiency of about 0.06 %.

PACS: 28.60.+s; 29.25.Rm

Keywords: Ion guide; On-line isotope separation

* Corresponding author. Tel.: +1-510-4867310; fax: +1-510-4867983. E-mail address: KPerajarvi@lbl.gov (K. Peräjärvi).

1. Introduction

Since several elements between Ca and Ni are refractory by their nature, their neutron-rich isotopes are rarely available as low energy Radioactive Ion Beams (RIB) in ordinary Isotope Separator On-Line (ISOL) facilities. The main ISOL work in this region of the chart of the nuclides has been done using quasi- and deep-inelastic reactions and solid catchers at GSI [1-3][†]. These low energy RIBs of refractory elements would be especially interesting to have available under conditions which allow high-resolution beta-decay spectroscopy, ion-trapping and laser-spectroscopy. As an example, availability of these beams would open a way for research which could produce interesting and important data on neutron-rich nuclei in the vicinity of the doubly magic ⁷⁸Ni.

One way to overcome the intrinsic difficulty of producing these beams is to rely on the chemically unselective Ion-Guide Isotope Separator On-Line (IGISOL) technique [5]. In general, in the existing IGISOL facilities, proton induced fission of actinides is the superior tool for the production of beams of neutron-rich nuclei down to about $A = 70$. However, production cross sections decrease rapidly below $A = 70$ [6]. One way to solve this problem is to rely on quasi- and deep-inelastic reactions, such as $^{197}\text{Au}(^{65}\text{Cu}, X)Y$, instead of fission. Before quasi- and deep-inelastic reactions can be successfully incorporated into the IGISOL concept, their kinematics must be well understood. The main complication with them, from the IGISOL point of view, is the high kinetic energy of the projectile like products. Also the energy distribution is relatively broad. These

[†] Recently, at the ISOLDE PSB facility at CERN, Mn beams were developed [4]. At ISOLDE the production of neutron-rich Mn isotopes is based on reactions induced by the 1 GeV proton beam hitting a 52 g/cm² UC_x/graphite target.

present difficulties since, in the conventional IGISOL technique, the reaction products finally thermalize into a relatively small volume filled with He-gas ($p_{\text{He}} \sim 300$ mbar). To evaluate this approach, the reaction kinematics part of this study was first performed at the Lawrence Berkeley National Laboratory (LBNL) using its 88" cyclotron and, based on these data, a specialized target chamber was built. This chamber was then moved to the Jyväskylä IGISOL facility for on- and off-line tests. In addition to the spectroscopy station, the Jyväskylä IGISOL facility is coupled to a double Penning trap ($m/\Delta m = 10^7$ - 10^8) and a laser spectroscopy installation. We wish to report the studies done both at Berkeley and Jyväskylä. First results from this project were briefly reported in [7]. For completeness, those findings will be repeated here.

2. Experimental setups and results

2.1 Quasi- and deep-inelastic reactions

The quasi- and deep-inelastic reactions which were investigated were $^{197}\text{Au}(^{55}\text{Mn},\text{X})\text{Y}$ and $^{197}\text{Au}(^{65}\text{Cu},\text{X})\text{Y}$. These reactions were studied using the LBNL 88" cyclotron and a large scattering chamber [8]. The $^{55}\text{Mn}^{+13}$ and $^{65}\text{Cu}^{+17}$ beams were produced using the ECR-ion source and they were accelerated up to 341 and 403 MeV final energies, respectively. Beam intensities on target ranged up to a few pA. To achieve optimum experimental conditions (the beam hitting perpendicularly on the target and a small beam spot (about $2 \text{ mm} \times 5 \text{ mm}$)), two collimators were installed upstream of the target ladder. The target ladder held three Au targets: 1.5, 1.93 and 2.6 mg/cm^2 . A ΔE (thickness 13 μm) – E (thickness 150 μm) Si-detector telescope was mounted about 15 cm from the target in a movable arm, behind a $2 \text{ mm} \times 5 \text{ mm}$ collimator. An additional Si E-detector

(thickness 500 μm), which served as a beam monitor, was mounted in a second movable arm at about the same distance from the target. To be able to generate an adequate understanding of the kinematics of the desired reactions, several measurements at angles from 30° to 70° in the laboratory frame of reference were performed. The master-trigger of the VME based data acquisition was a logical OR between the monitoring counter and a logical AND of the ΔE -E detectors. The energy calibration of the detectors was done using calibrated precision pulsers and the elastically scattered beam particles.

As an example of the quality of the reaction data, Fig. 1a and e represent the $\Delta E - E$ matrix measured at 60° in the laboratory for both the ^{65}Cu and ^{55}Mn beams. As shown in Fig. 1b and e, with these two primary beams, one is able to cover all elements from Zn down to Sc. Figure 1c illustrates the total energy distributions at 60° for the products that have $Z < 29$ and $Z < 27$. The energy distributions have different shapes since the quasi-elastic channel is more open with the Ni and Co isotopes than with Fe, Mn etc. Figure 1d presents the angular distributions of the projectile like quasi- and deep inelastic reaction products ($Z < 29$ and $Z < 27$) observed by bombarding a 1.5 mg/cm^2 thick ^{197}Au target with 403 MeV ^{65}Cu ions.

2.2. *Specialized target chamber*

Various compromises influenced the design of this specialized IGISOL target chamber. Primarily, in this first trial with quasi- and deep inelastic reactions, we did not want to deviate too much from the optimized Heavy Ion-Guide Isotope Separator On-Line (HIGISOL) parameters [9]. As an example, the thicker the target becomes, the more one

needs to worry about beam scattering and heating. So, about a 3.0 mg/cm^2 Au-target was a safe choice. Secondly, thermalization of the reaction products was facilitated by keeping the cyclotron beam energy as low as possible, but always high enough to exceed the Coulomb barrier. In case of ^{65}Cu this lead to about 403 MeV beam energy when it penetrates the Au target. However, for future studies, it is important to note that the total deep-inelastic cross section increases as a function of energy, and with this higher energy, more deep inelastic channels open up [10, 11].

Based on the reaction measurements introduced in section 2.1 and the above discussion, the angular acceptance of the stopping volume of the new target chamber was selected to lie between 40 to 70 degrees, see Figs. 1d and 2. As also shown in Fig. 2, the stopping volume is separated from the primary beam using a Ni-window to decrease the plasma density. (This approach is also used in the fission [12] and the HIGISOL [9] target chambers.) Reaction data also lead to a 9.0 mg/cm^2 thick Ni window for the above conditions. The purpose of the slow He flow through the target volume using the connecting channel and the second exit hole is to cool the Au-target and the Havar-windows. This simplifies the rest of the design since it eliminates the need for water cooling the target and windows. The rest of the constraints on the design of the target chamber came from the dimensions of the existing IGISOL front-end parts such as: collimators, He-lines, skimmer, etc. A photo of the chamber is shown in Fig. 3.

2.3. On- and off-line studies at Jyväskylä

The $^{197}\text{Au}(^{65}\text{Cu},\text{X})\text{Y}$ reaction was used in the on-line experiment at Jyväskylä. That was mostly because the ^{65}Cu beam was already developed and in use at Jyväskylä and secondly because this reaction synthesizes nuclei closer to $A = 70$ line. The Au target used had a thickness of about 3 mg/cm^2 and the initial $^{65}\text{Cu}^{+15}$ beam energy was about 443 MeV. This beam slows down to about 403 MeV in the entrance Havar window and the He gas. A small fraction of the projectile like reaction products recoiling out from the Au target could be converted to a low energy +1 ion beam using the target chamber introduced in section 2.2. The +1 ion beam was separated from the neutral gas, accelerated up to 40 keV kinetic energy, mass-separated and transported into the experimental area using the existing IGISOL installation [13]. Mass separated RIBs were implanted into a movable tape viewed by a coaxial HPGe detector (70 % relative efficiency) and two ion implanted Si-detectors (thickness 500 μm). The master trigger of the VME based data acquisition system was a logical OR of all the detectors. The energy and the efficiency calibration of the HPGe detector were mainly based on ^{60}Co , ^{106}Ru , ^{133}Ba , ^{134}Cs and ^{137}Cs sources. The total beta-efficiency was determined using the on-line data.

In addition to the above on-line setup, for off-line tests a ^{223}Ra alpha-recoil source (collected onto the tip of a needle) was placed inside the target chamber between the He-inlet channel and the stopping volume (at the opposite side of the stopping volume compared to the exit-hole). Emitted ^{219}Rn alpha-recoils were then used for transport efficiency studies. The resulting mass separated 40 keV ^{219}Rn ion beam was implanted

into a thin C-foil viewed by a single ion implanted Si-detector (thickness 500 μm). The data generated by this Si-detector were collected using a separate multi channel analyzer system.

Figure 4 shows a part of the beta-gated gamma-spectrum of $A = 63$ reaction products. The 87 keV gamma transition belonging to the beta-decay of ^{63}Co is clearly seen. In addition to establishing the yield (using gamma-singles data), this transition was used to determine the absolute beta-efficiency of 2.3(6) % for the pair of Si-detectors. Despite the modest beta-efficiency, we were able to measure the yields shown in Fig. 5.

3. Analysis of the experimental data

In order to evaluate the total IGISOL efficiency the cross section for Co isotopes emitted between 40 and 70 degrees is needed. This cross section was determined using the reaction data to be about 96 mbarn. By combining that result with the data provided by the large acceptance magnetic spectrometer PRISMA [14, 15], one can estimate the isotopic cross sections for different Co isotopes.

As shown in Fig. 5 the yields of mass-separated radioactive projectile-like species such as $^{62,63}\text{Co}$ are about 0.8 ions/s/pnA. By combining these yields with the cross section data, we can get an estimate of the total IGISOL efficiency for the products that penetrate the Ni-window of about 0.06 %. The maximum beam intensity normally available at Jyväskylä for a 443 MeV $^{65}\text{Cu}^{+15}$ beam is about 20 pnA. Because of some vacuum problems in the ECR-ion source, we were not able to go above 6 pnA in this experiment; the total IGISOL efficiency was determined using about a 4 pnA beam intensity.

However, based on the earlier HIGISOL studies [16], one can assume that the total efficiency remains more or less constant up to the maximum ^{65}Cu beam intensity available. This total IGISOL efficiency is a product of two coupled loss factors, namely inadequate thermalization and the intrinsic IGISOL efficiency. In our chamber, about 9 % of the Co-recoils were thermalized in the flowing He-gas ($p_{\text{He}} = 300$ mbar) and about 0.7 % of these were converted into a mass-separated ion beam. This intrinsic IGISOL efficiency is comparable to the one reported in [16] for the HIGISOL system (0.5 %). Figure 6 presents the measured yields for $^{62,63}\text{Co}$ as a function of ^{65}Cu beam energy. As expected, clear maxima at 443 MeV are observed.

A calibrated ^{223}Ra alpha-recoil source was used to further investigate the intrinsic IGISOL efficiency. Absolute intrinsic efficiencies of about 1.3 % for the ^{219}Rn alpha-recoils from the source position through the whole system (without the cyclotron beam) were measured ($p_{\text{He}} = 200$ mbar). When a 2.7 pA ^{65}Cu beam was switched on, the transport efficiency dropped by a factor of five. These efficiencies are comparable to the ones published in [17] for a long cylindrically symmetric gas cell which suggests a relatively “direct” and fast flow channel between the source position and the exit hole. This analysis was verified with the He-flow simulations shown in Fig. 7. These flow simulations were done using a COSMOS FloWorks 2004 code, SP0, standard edition [18]. These simulations also show a relatively smooth overall evacuation of the chamber.

5. Conclusions

It has been shown for the first time that quasi- and deep-inelastic reactions can be successfully incorporated into the conventional IGISOL technique. In the future, both of the primary physical/chemical loss mechanisms (thermalization and intrinsic IGISOL efficiency) can be suppressed by introducing Ar as a buffer gas and by relying on selective laser re-ionization. This combination will produce isobarically pure beams and it will increase the existing yields by at least a factor of 100, making this overall approach to the study of neutron rich nuclei quite attractive. Several cyclotron beam development projects, such as the development of a ^{55}Mn beam, are currently in progress at Jyväskylä. When completed, they will offer additional possibilities for this type of application. Also, the formation of IGISOL beams of target like products as well as dedicated studies with higher cyclotron beam energies can be considered. From the IGISOL technique point of view, it would be of interest to study further the alpha-recoil efficiency and the on-line intrinsic efficiency as a function of beam intensity.

Acknowledgements

This work was supported by the Director, Office of Science, Nuclear Physics, U.S. Department of Energy under Contract No. DE-AC03-76SF00098. We also thank the Academy of Finland for financial support and the European Union for experimental access via its Large Scale Facilities programme.

References

- [1] E. Runte et al., Nucl. Phys. A399 (1983) 163.

- [2] E. Runte et al., Nucl. Phys A441 (1985) 237.
- [3] U. Bosch et al., Nucl. Phys. A477 (1988) 89.
- [4] M. Hannawald et al., Phys. Rev. Lett. 82 (1999) 1391.
- [5] J. Äystö, Nucl. Phys. A 693 (2001) 477.
- [6] M. Huhta et al., Physics Letters B 405 (1997) 230.
- [7] K. Peräjärvi et al., Eur. Phys. J. A, to be published.
- [8] F. Guo, Ph.D. thesis, Nuclear Reactions with ^{11}C and ^{14}O Radioactive Ion Beams, University of California, Berkeley, 2004.
- [9] R. Béraud et al., Nucl. Instr. and Meth. A 346 (1994) 196.
- [10] J. Péter et al., Nucl. Phys. A 279 (1977) 110.
- [11] L. Moretto, private communication.
- [12] P. Taskinen et al., Nucl. Instr. and Meth. A 281 (1989) 539.
- [13] H. Penttilä et al., Eur. Phys. J. A, to be published.
- [14] A. Gadea et al., Eur. Phys. J. A, to be published.
- [15] A. Gadea et al., Eur. Phys. J. A 20 (2004) 193.
- [16] P. Dendooven et al., Nucl. Instr. and Meth. A 408 (1998) 530.
- [17] K. Peräjärvi et al., Nucl. Phys. A 701 (2002) 570c.
- [18] <http://www.cosmosfloworks.com>

Figure captions

Fig. 1. (a) ΔE -E graph for the 403 MeV $^{65}\text{Cu} + ^{197}\text{Au}$ (1.5 mg/cm^2) reaction at 60 degrees, (b) ΔE gated by gate 1 in (a), (c) $\Delta E + E$ gated by gate 2 and 3 in (a), (d) Angular distributions of projectile like reaction products $Z < 29$ and $Z < 27$, (e) $\Delta E - E$ graph for the 341 MeV $^{55}\text{Mn} + ^{197}\text{Au}$ (1.5 mg/cm^2) reaction at 60 degrees.

Fig. 2. Target chamber designed for use with quasi- and deep-inelastic reactions. The parts of the chamber are: 1) Havar-windows (1.8 mg/cm^2), 2) Au-target (3.0 mg/cm^2 , diameter = 7 mm), 3) Conical Ni-window (9.0 mg/cm^2 , angular acceptance from 40 to 70 degrees), 4) He-inlet, 5) Stopping volume, 6) Exit-hole ($d = 1.2 \text{ mm}$), 7) Connecting channel ($d = 1 \text{ mm}$), 8) Second exit-hole ($d = 0.3 \text{ mm}$), 9) Skimmer electrode.

Fig. 3. A photograph presenting the different components of the chamber. Arrows indicate how the major parts are assembled.

Fig. 4. Part of the beta-gated gamma spectrum of $A = 63$.

Fig. 5. Measured yields in units of ions/s/pnA for the ^{65}Cu on ^{197}Au reaction. The cyclotron beam energy in the different measurements is also shown.

Fig. 6. The yields for $^{62,63}\text{Co}$ as a function of ^{65}Cu beam energy.

Fig. 7. Simulated He-flow field in the stopping volume. Solid lines correspond to the computed tracks of macroscopic flow particles. The line color is related to the local flow velocity.

Fig. 1.

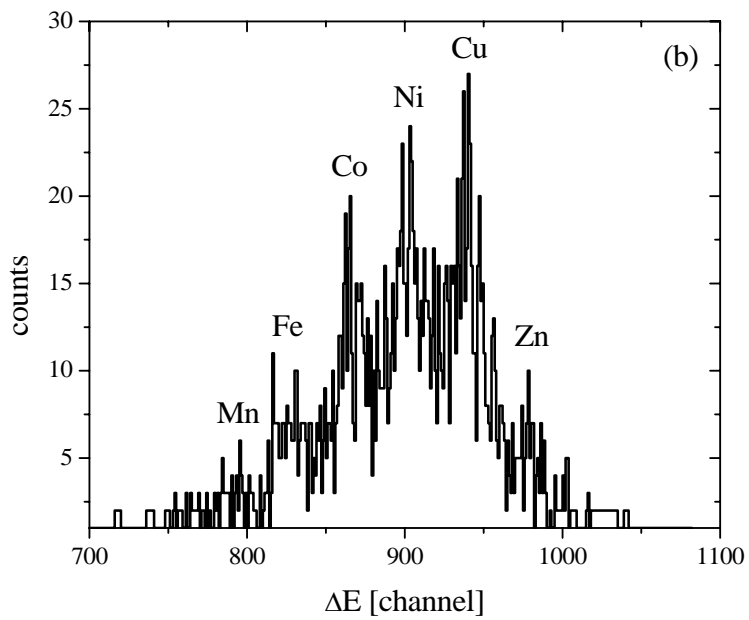
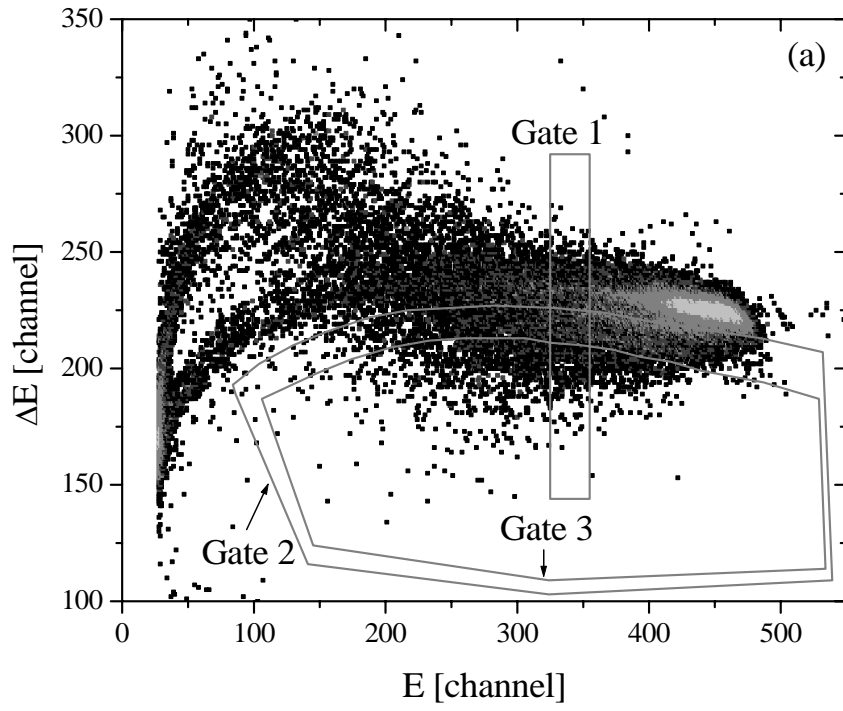


Fig. 1.

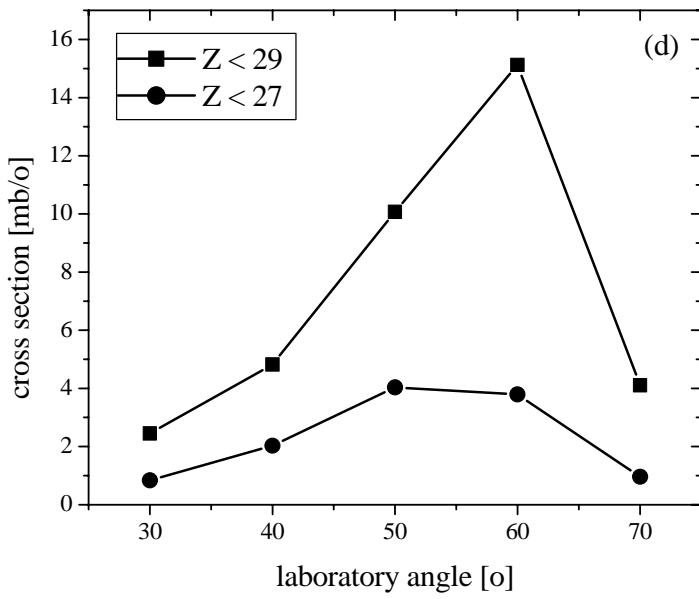
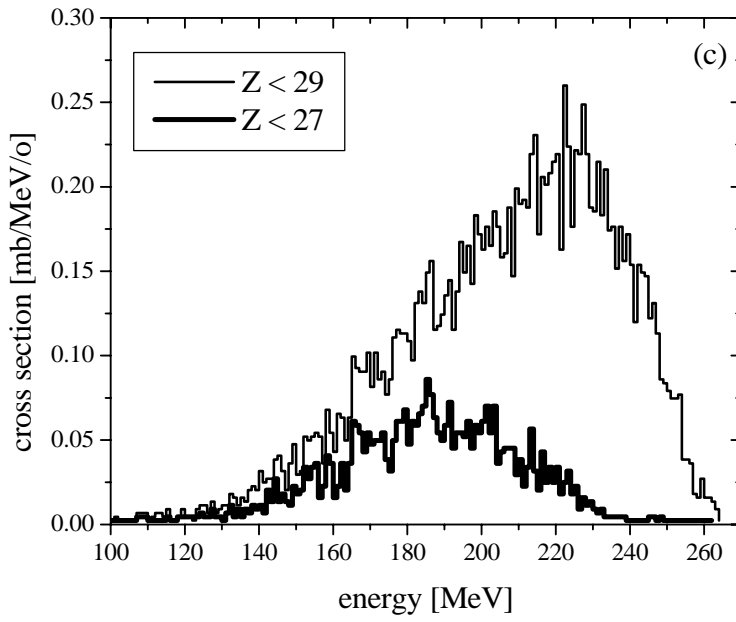


Fig. 1.

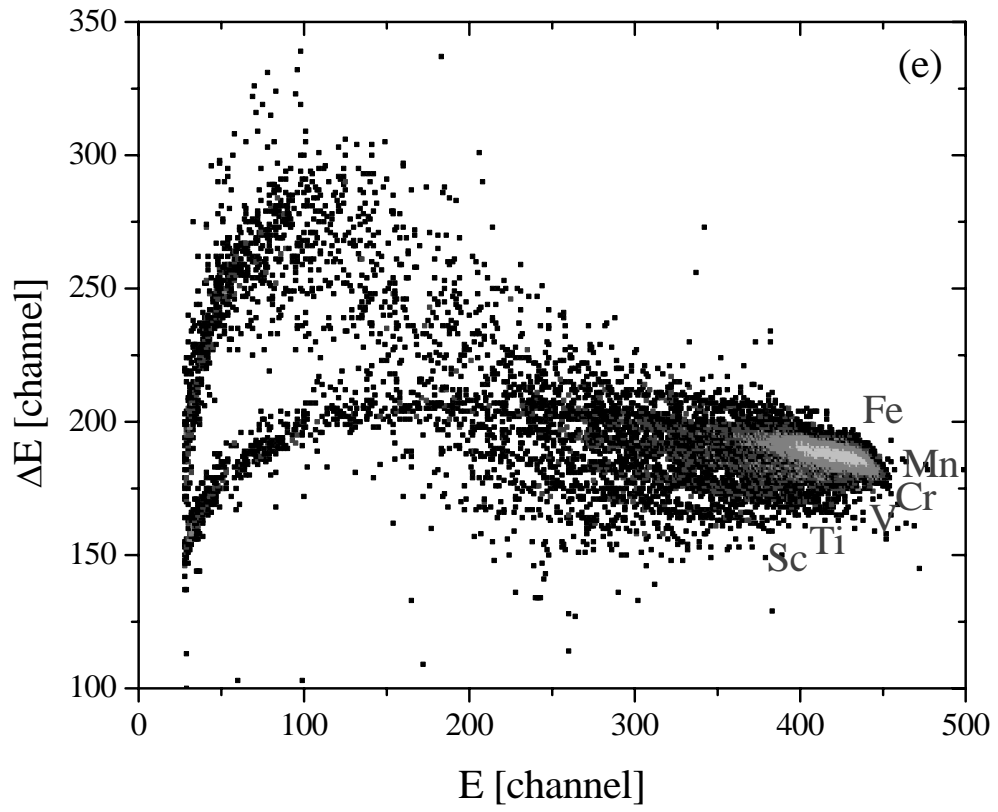


Fig. 2.

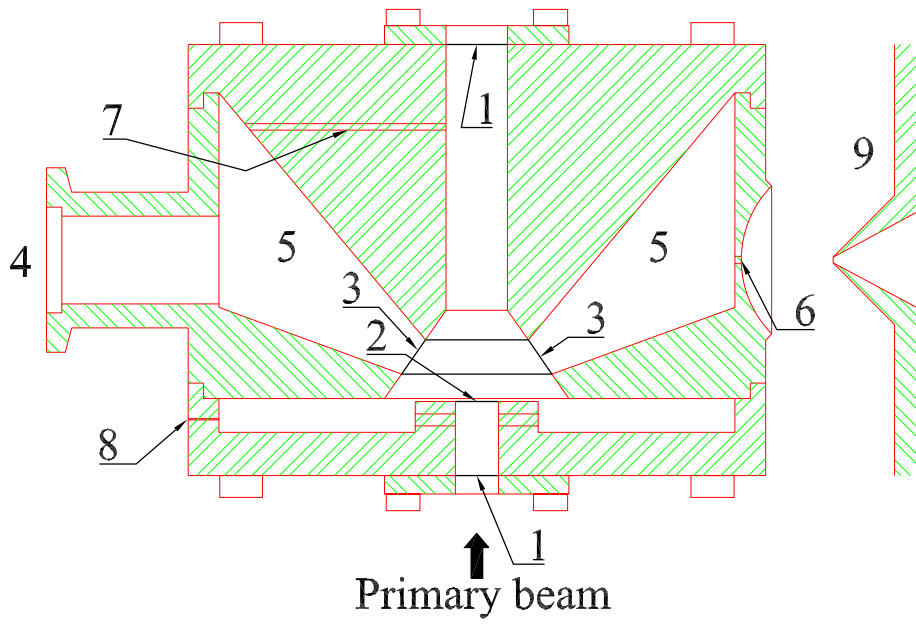


Fig. 3.

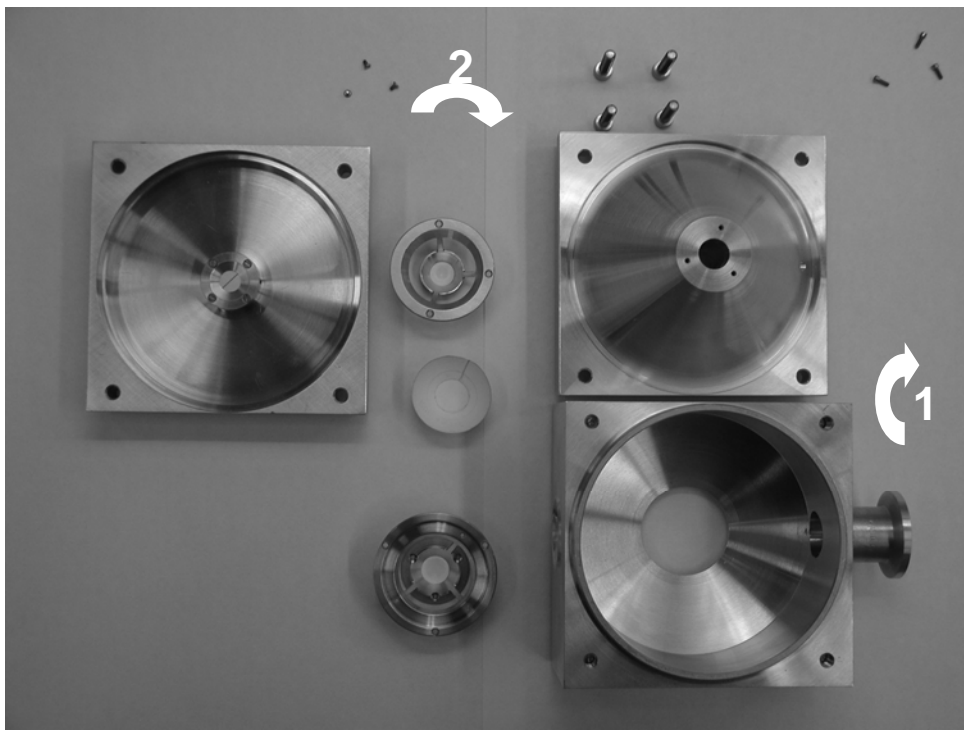


Fig. 4.

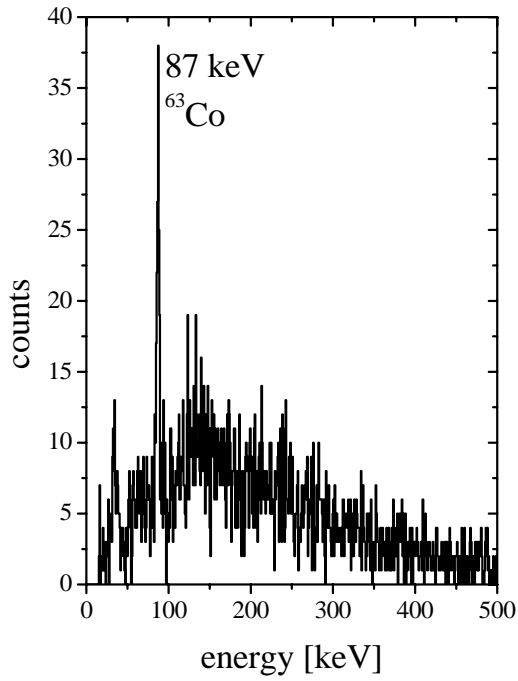


Fig. 5.

^{65}Cu Beam				
^{62}Ni 3.634	^{63}Ni 100 a	^{64}Ni 0.926	^{65}Ni 2.52 h	^{66}Ni 54.6 h
^{61}Co 1.65 h	^{62}Co 14.0, 1.5 min 0.9 443 MeV	^{63}Co 27.5 s 0.8 443 MeV	^{64}Co 0.3 s 0.3 443 MeV	
^{60}Fe 1.5×10^6 a	^{61}Fe 6.0 min 0.2 423 MeV	^{62}Fe 68 s <0.02 423 MeV		
^{59}Mn 4.6 s				

Fig. 6.

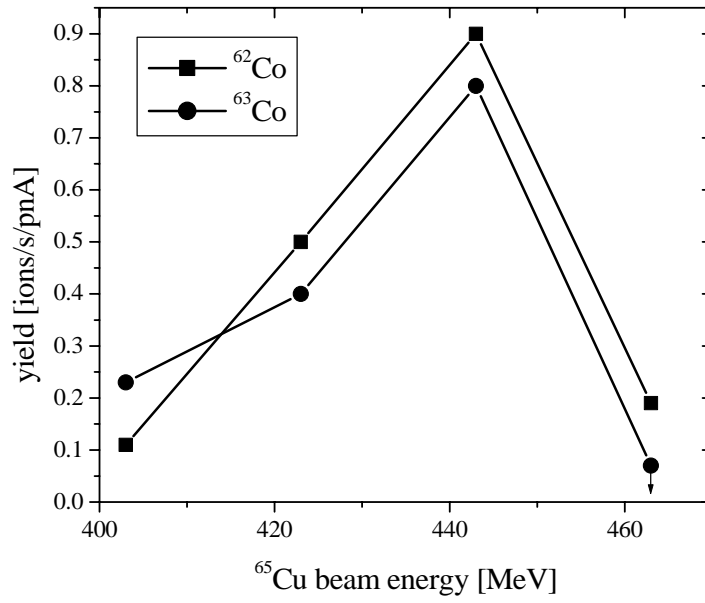


Fig. 7.

